Dimethyl Ether Synthesis with in situ H_2O Removal in Fixed-Bed Membrane Reactor: Model and Simulations[†]

I. Iliuta, F. Larachi,* and P. Fongarland[‡]

Department of Chemical Engineering, Laval University, Québec, G1 V 0A6, Canada

The potential and limits of in situ removal of water under dimethyl ether (DME) synthesis conditions in a fixed-bed membrane reactor were studied numerically. The motivation for in situ H_2O removal during DME synthesis by means of hydrophilic membranes is to displace the water−gas shift equilibrium to enhance conversion of CO_2 into methanol to improve DME productivity. In CO-rich feeds, methanol yield/selectivity increases/decreases slowly with increasing H_2O permeance because only small amounts of water are removed from the system. Methanol dehydration is not inhibited by water, and DME selectivity is not improved significantly with increasing H_2O permeance. When CO is gradually replaced with CO_2, with the increase of H_2O membrane permeance and H_2O removal, methanol yield and DME selectivity are favored and the fraction of unconverted methanol is reduced as the dehydration reaction is accelerated due to reduced kinetic inhibition by H_2O.

Introduction

Syngas conversion into liquid chemicals such as methanol, fuel products, and oxygenates is a very active area mobilizing important academic and industrial resources, especially for energy densification from remote natural gas sources or for clean coal conversion. In this context, the synthesis of dimethyl ether has received over the past decade growing attention for its potential as a substitute to automotive and cooking fuels.[1−9] DME thermal efficiency being equivalent to traditional diesel fuel has recently been suggested as an alternative fuel for diesel engines, in addition to reduction of NO_x emissions and near-zero smoke production. DME can also be used as an intermediate for the synthesis of other chemicals, such as dimethyl sulfate or lower olefins.

Direct synthesis of DME from syngas is reversible and exothermic.[9] It involves two steps, i.e., methanol synthesis followed by in situ methanol dehydration (eqs 1−3). This reaction requires two independent catalysis functions: methanol forming and dehydration functions. An advantage inherent to the coproduction of the (methanol−DME) tandem is an alleviation of the thermodynamic equilibrium constraint by the methanol synthesis step[7] which results in an increased oxygenates productivity. Water−gas shift (WGS) can be used as a "chemical wheel" and offers the system an extra kinetic flexibility by lowering water build-up to accelerate methanol dehydration. WGS also allows providing more hydrogen especially for H_2-poor syngas feeds as those originating from biomass or coal gasification.

Methanol synthesis reaction

$$CO_2 + 3H_2 \leftrightarrow CH_3OH + H_2O \quad (1)$$

Water−gas shift reaction

$$CO + H_2O \leftrightarrow H_2 + CO_2 \quad (2)$$

Methanol dehydration reaction

$$2CH_3OH \leftrightarrow CH_3OCH_3 + H_2O \quad (3)$$

Overall reaction

$$3CO + 3H_2 \leftrightarrow CH_3OCH_3 + CO_2 \quad (4)$$

A methanol synthesis catalytic function operating on reactions 1 and 2 is combined with an acidic catalytic function to enable reaction 3. Depending on operating conditions, reactions 1−3 highlight some synergistic effects that can be taken advantage of to improve methanol conversion into DME. Hence, methanol consumption via reaction 3 can be doubly stimulated via WGS 2: by the consumption of water (itself resulting from reactions 1 and 3) and by the generation of hydrogen to drive methanol production via reaction 1.[9]

A strong synergy is obtained using CO-rich feeds due to effective removal of water via WGS and of methanol via dehydration.[4] Unfortunately, CO_2-rich feeds promote reverse WGS which attenuates synergy because of H_2O accumulation from reactions 1 and 2.[4] Selectivity to methanol or DME is always favored at the two opposite extremes of feed composition.[4] With CO-rich feeds and where dehydration is not affected by H_2O, DME conversion is favored. Conversely, CO_2-rich feeds favor high fractions of unconverted methanol due to large quantity of H_2O produced in methanol synthesis and dehydration steps thus inhibiting methanol dehydration and DME selectivity. Thus, it is anticipated that H_2O in situ removal during DME synthesis may bring some beneficial effects: at high CO_2 content, in situ H_2O removal accelerates the reverse water gas shift reaction of CO_2 with H_2 toward CO,[10] which is expected to improve DME production;[7,11] in the case of H_2-rich synthesis gas, in situ H_2O removal would favor DME selectivity.[9] Studies on the effect of water in the DME reaction medium were discussed by numerous investigators.[4,11−14]

Removal of water in syngas-mediating reactions can be effected by several means such as interstage cooling and condensation, adsorption, or membranes. Its removal using hydrophilic (zeolite, amorphous, or polymer) membranes was tested in slurry, fixed-bed, or fluidized-bed reactors for

[†] Part of the Professor Hugo de Lasa Festschrift.

* To whom correspondence should be addressed. E-mail: faical.larachi@gch.ulaval.ca.

[‡] Ecole Centrale de Lille, Unité de Catalyse et Chimie du Solide, 59655 Villeneuve d'Ascq Cedex, France.

10.1021/ie901726u
Published on Web 02/08/2010

Fischer−Tropsch synthesis, in which integration of sufficiently large membrane areas can enable fast removal of incipient H_2O.[10] Membranes are swept using a sweep gas (N_2 from ASU or desulfurized natural gas) at low pressure to ensure a sufficient transmembrane driving force. These should be highly permeable toward H_2O while preferably retaining H_2, CO, CO_2, and hydrocarbons almost completely in the retentate section to avoid additional downstream recovery. In practice, such water selective removal will require high membrane permeances, permselectivity to water, and also high resilience.

Application of hydrophilic membranes to enhance the productivity of Fischer−Tropsch synthesis (FTS) reactors was proposed by Espinoza et al.[15] Their results suggest high H_2O fluxes and reasonable H_2O/H_2 and H_2O/hydrocarbons separation factors. Rohde and co-workers[16,17] experimentally demonstrated the feasibility of in situ H_2O removal under FTS conditions in lab-scale fixed-bed membrane reactors using hydrophilic amorphous silica and supported polymer membranes. The potential of combining a membrane with an FTS reactor was also illustrated through simulations.[10] It was shown that the performance of the fixed-bed membrane reactor under FTS conditions depends on the choice of the sweep gas, while minimum membrane requirements with regard to in situ H_2O removal were formulated. Microporous zeolite membranes were reported to outperform both amorphous microporous and polymer membranes in terms of permeance and permselectivity. Simulated case studies on in situ H_2O removal revealed a significant potential for catalyst protection in cobalt-based FTS and for conversion enhancement in iron-based FTS catalysis.

The motivation for in situ H_2O removal during DME synthesis by means of hydrophilic membranes is to accelerate methanol production by increasing reactant partial pressures and/or by reducing kinetic inhibition by H_2O while shifting WGS so as to favor CO formation. By applying this concept, CO_2 can be utilized as a syngas constituent as in situ H_2O removal accelerates reverse WGS which would legitimate the extension of the membrane-based syngas catalysis from Fischer−Tropsch to DME synthesis. To the best of our knowledge, the selective removal of H_2O from a mixture of H_2, CO, CO_2, CH_3OCH_3, and CH_3OH under DME synthesis conditions has not been attempted yet using combined membrane−fixed-bed reactor systems. This work therefore intends to analyze through modeling and simulations such extension in order to evaluate the potential and limits of in situ H_2O removal under DME synthesis conditions in a fixed-bed membrane reactor and a low inlet H_2/CO ratio.

Membrane Fixed-Bed Reactor Model

A chemical reaction engineering model for a fixed-bed membrane reactor was elaborated to evaluate the potential and limits of the concept of H_2O removal during DME synthesis. An isothermal 1D unsteady-state, plug-flow reactor model was assumed for both permeate and retentate sections. The retentate compartment is packed with bifunctional catalytic particles for DME production from H_2-CO_x (i.e., CO + CO_2) whereas the permeate section is an empty cavity swept by an inert gas. The local j species molar fluxes in the streamwise direction in both compartments are determined by the rates of transmembrane transport and reaction in the retentate catalytic bed. The transmembrane molar flux of any j species is proportional to the j species partial pressure difference across membrane and permeance, and to membrane area.[10] Only water and hydrogen were assumed to get involved in transmembrane transits. A zeolite membrane was used assuming H_2O permeances ranging from 10^{-10} to 5×10^{-10} kmol/(s m^2 Pa) and H_2O/H_2 permselectivity >10 at 250 °C.[10]

Mass and Momentum Transport Conservation Equations. The unsteady-state mass and momentum balance equations for the fixed-bed (retentate section) and permeate sides are formulated below. To avoid burdening the text with the meaning of all the variables intervening in these equations, the Nomenclature section can be consulted.

• Species conservation equations for fixed-bed side

$$\varepsilon_g \frac{\partial}{\partial t}(C_{H_2}) + \varepsilon_g \frac{\partial}{\partial z}(u_g C_{H_2}) + \rho_{sc}(3r_1 - r_2) + \frac{A}{V_r} Q_{H_2}(p_{H_2} - \tilde{p}_{H_2}) = 0 \quad (5)$$

$$\varepsilon_g \frac{\partial}{\partial t}(C_{CO_2}) + \varepsilon_g \frac{\partial}{\partial z}(u_g C_{CO_2}) + \rho_{sc}(r_1 - r_2) = 0 \quad (6)$$

$$\varepsilon_g \frac{\partial}{\partial t}(C_{H_2O}) + \varepsilon_g \frac{\partial}{\partial z}(u_g C_{H_2O}) - \rho_{sc}(r_1 - r_2 + r_3) + \frac{A}{V_r} Q_{H_2O}(p_{H_2O} - \tilde{p}_{H_2O}) = 0 \quad (7)$$

$$\varepsilon_g \frac{\partial}{\partial t}(C_{CO}) + \varepsilon_g \frac{\partial}{\partial z}(u_g C_{CO}) + \rho_{sc} r_2 = 0 \quad (8)$$

$$\varepsilon_g \frac{\partial}{\partial t}(C_{CH_3OH}) + \varepsilon_g \frac{\partial}{\partial z}(u_g C_{CH_3OH}) + \rho_{sc}(2r_3 - r_1) = 0 \quad (9)$$

$$\varepsilon_g \frac{\partial}{\partial t}(C_{CH_3OCH_3}) + \varepsilon_g \frac{\partial}{\partial z}(u_g C_{CH_3OCH_3}) - \rho_{sc} r_3 = 0 \quad (10)$$

• Global balance equation for fixed-bed side

$$\varepsilon_g \frac{\partial}{\partial t}(C_G) + \frac{\partial}{\partial z}(\dot{F}) + 2\rho_{sc} r_1 + \frac{A}{V_r} Q_{H_2}(p_{H_2} - \tilde{p}_{H_2}) + \frac{A}{V_r} Q_{H_2O}(p_{H_2O} - \tilde{p}_{H_2O}) = 0 \quad (11)$$

• Species conservation equations for permeate side (H_2, H_2O, inert sweep gas)

$$\tilde{\varepsilon}_g \frac{\partial}{\partial t}(\tilde{C}_{H_2}) + \tilde{\varepsilon}_g \frac{\partial}{\partial z}(\tilde{u}_g \tilde{C}_{H_2}) - \frac{A}{V_r} Q_{H_2}(p_{H_2} - \tilde{p}_{H_2}) = 0 \quad (12)$$

$$\tilde{\varepsilon}_g \frac{\partial}{\partial t}(\tilde{C}_{H_2O}) + \tilde{\varepsilon}_g \frac{\partial}{\partial z}(\tilde{u}_g \tilde{C}_{H_2O}) - \frac{A}{V_r} Q_{H_2O}(p_{H_2O} - \tilde{p}_{H_2O}) = 0 \quad (13)$$

$$\tilde{\varepsilon}_g \frac{\partial}{\partial t}(\tilde{C}_i) + \tilde{\varepsilon}_g \frac{\partial}{\partial z}(\tilde{u}_g \tilde{C}_i) = 0 \quad (14)$$

• Global balance equation for permeate side

$$\tilde{\varepsilon}_g \frac{\partial}{\partial t}(\tilde{C}_G) + \frac{\partial}{\partial z}(\dot{\tilde{F}}) - \frac{A}{V_r} Q_{H_2}(p_{H_2} - \tilde{p}_{H_2}) - \frac{A}{V_r} Q_{H_2O}(p_{H_2O} - \tilde{p}_{H_2O}) = 0 \quad (15)$$

• Momentum balance equations for fixed-bed and permeate sides

$$\frac{\partial}{\partial t}(\rho_g \varepsilon_g u_g) + u_g \frac{\partial}{\partial z}(\rho_g \varepsilon_g u_g) = - \varepsilon_g \frac{\partial P}{\partial z} - \left[E_1 \frac{(1-\varepsilon_g)^2}{\varepsilon_g^3 d_p^2}\mu_g v_{sg} + E_2 \frac{1-\varepsilon_g}{\varepsilon_g^3 d_p}\rho_g v_{sg}^2\right]\varepsilon_g - \frac{A}{V_r}\frac{zRT}{P}(y_{H_2} + y_{H_2O})^{-1}[Q_{H_2}(p_{H_2} - \tilde{p}_{H_2}) + Q_{H_2O}(p_{H_2O} - \tilde{p}_{H_2O})] [Q_{H_2}M_{H_2}(p_{H_2} - \tilde{p}_{H_2}) + Q_{H_2O}M_{H_2O}(p_{H_2O} - \tilde{p}_{H_2O})] \quad (16)$$

$$\frac{\partial}{\partial t}(\tilde{\rho}_g \tilde{\varepsilon}_g \tilde{u}_g) + \tilde{u}_g \frac{\partial}{\partial z}(\tilde{\rho}_g \tilde{\varepsilon}_g \tilde{u}_g) = -\tilde{\varepsilon}_g \frac{\partial \tilde{P}}{\partial z} + \frac{A}{V_p}\frac{zRT}{P} \times (y_{H_2} + y_{H_2O})^{-1}[Q_{H_2}(p_{H_2} - \tilde{p}_{H_2}) + Q_{H_2O}(p_{H_2O} - \tilde{p}_{H_2O})] [Q_{H_2}M_{H_2}(p_{H_2} - \tilde{p}_{H_2}) + Q_{H_2O}M_{H_2O}(p_{H_2O} - \tilde{p}_{H_2O})] \quad (17)$$

• Peng−Robinson EOS for multicomponent systems[18]

$$Z_i^3 - (1 - B_i)Z_i^2 + (A_i - 2B_i^2 - 2B_i)Z_i - (A_iB_i - B_i^3 - B_i^2) = 0 \quad (18)$$

where

$$i = r; \quad Z_r = P\varepsilon_g u_g/RT\dot{F}; \quad A_r = Pa/(RT)^2; \quad B_r = Pb/RT \quad (19)$$

$$i = p; \quad Z_p = \tilde{P}\tilde{\varepsilon}_g \tilde{u}_g/RT\dot{\tilde{F}}; \quad A_p = \tilde{P}a/(RT)^2; \quad B_p = \tilde{P}b/RT \quad (20)$$

The values of the parameters a and b were calculated from the critical properties of each component in the mixture. The following mixing rules are used to evaluate a an b for mixtures of pure components:

$$a = \sum\sum y_i y_j a_{ij} \quad (21)$$

$$a_j = \sum y_i a_{ij} \quad (22)$$

$$a_{ij} = (a_i' a_j')^{1/2}(1 - \kappa_{ij}) \quad (23)$$

$$a_j' = a_{cj}\alpha_j \quad (24)$$

$$a_{cj} = 0.45724[(RT_{cj})/P_{cj}] \quad (25)$$

$$\alpha_j = [1 + m_j(1 - (T/T_{cj})^{1/2})]^2 \quad (26)$$

$$m_j = 0.384401 + 1.522760\omega - 0.213808\omega^2 + 0.034616\omega^3 - 0.001976\omega^4 \quad (27)$$

$$b = \sum y_j b_j \quad (28)$$

$$b_j = 0.077796(RT_{cj}/P_{cj}) \quad (29)$$

Here P ($\tilde{P}$), ε_g ($\tilde{\varepsilon}_g$), ρ_g ($\tilde{\rho}_g$), and u_g ($\tilde{u}_g$) represent, respectively, pressure, void volume fraction, gas density, and interstitial gas velocity for the fixed bed and permeate sides, respectively. The second term in the right side of eq 16 represents the interfacial drag force per unit reactor volume, and the third term, the membrane sweep-momentum. C_j ($\tilde{C}_j$) represents the mole concentration of species j in the fixed-bed or permeate side; Q_j and A are, respectively, the membrane j species permeance and area.

DME Synthesis Kinetics. The kinetics of DME synthesis reactions in a fixed-bed reactor with Cu−ZnO−Al_2O_3/HZSM-5 catalyst[9] for methanol synthesis (Cu−ZnO−Al_2O_3) and for methanol dehydration (HZSM-5) was used to evaluate the potential and limits of in situ H_2O removal under DME synthesis. With the terms of methanol and water adsorption neglected, the kinetic equations are the following:[9]

$$r_1 = K_1 \frac{p_{CO_2}p_{H_2}\left(1 - \frac{1}{K_{p,1}}\frac{p_{H_2O}p_{CH_3OH}}{p_{CO_2}p_{H_2}^3}\right)}{(1 + K_{CO_2}p_{CO_2} + K_{CO}p_{CO} + \sqrt{K_{H_2}p_{H_2}})^3} \quad (30)$$

$$r_2 = K_2 \frac{p_{H_2O} - \frac{1}{K_{p,2}}\frac{p_{CO_2}p_{H_2}}{p_{CO}}}{(1 + K_{CO_2}p_{CO_2} + K_{CO}p_{CO} + \sqrt{K_{H_2}p_{H_2}})} \quad (31)$$

$$r_3 = K_3\left(\frac{p_{CH_3OH}^2}{p_{H_2O}} - \frac{p_{CH_3OCH_3}}{K_{p,3}}\right) \quad (32)$$

where the kinetic,[9] adsorption,[2,19] and equilibrium[19,20] constants are

$$K_1 = 35.45\exp\left(-\frac{1.7069 \times 10^4}{RT}\right), \text{ kmol/(kg}_{cat}\text{ s bar}^2) \quad (33)$$

$$K_2 = 7.3976\exp\left(-\frac{2.0436 \times 10^4}{RT}\right), \text{ kmol/(kg}_{cat}\text{ s bar)} \quad (34)$$

$$K_3 = 8.2894 \times 10^4\exp\left(-\frac{5.2940 \times 10^4}{RT}\right), \text{ kmol/(kg}_{cat}\text{ s bar)} \quad (35)$$

$$K_{H_2} = 0.249\exp\left(\frac{3.4394 \times 10^4}{RT}\right), \text{ 1/bar} \quad (36)$$

$$K_{CO_2} = 1.02 \times 10^{-7}\exp\left(\frac{6.74 \times 10^4}{RT}\right), \text{ 1/bar} \quad (37)$$

$$K_{CO} = 7.99 \times 10^{-7}\exp\left(\frac{5.81 \times 10^4}{RT}\right), \text{ 1/bar} \quad (38)$$

$$\ln K_{p,1} = 4213/T - 5.752\ln T - 1.707 \times 10^{-3}T + 2.682 \times 10^{-6}T^2 - 7.232 \times 10^{-10}T^3 + 17.6 \quad (39)$$

$$\log K_{p,2} = 2167/T - 0.5194\log T + 1.037 \times 10^{-3}T - 2.331 \times 10^{-7}T^2 - 1.2777 \quad (40)$$

$$\ln K_{p,3} = 4019/T + 3.707\ln T - 2.783 \times 10^{-3}T + 3.8 \times 10^{-7}T^2 - 6.56 \times 10^4/T^3 - 26.64 \quad (41)$$

Results and Discussion

A series of simulations at 250 °C and 5 MPa without in situ H_2O removal was first carried out to investigate the dependence of kinetics of DME synthesis on CO_2 content of the feed gas to assist CO_2 management in the process and to give a suitable database for refinement of the DME model. Then, under the same temperature and pressure conditions, the potential and limits of in situ H_2O removal under DME synthesis conditions were studied. Fixed-bed membrane reactor operating conditions for the base case are listed in Table 1.

No in situ H_2O Removal. The simulation results without in situ H_2O removal are first examined. Figure 1 shows typical steady-state methanol yield profiles obtained through gradually replacing CO_2 by CO for $H_2/CO_x = 1$ and $H_2/CO_x = 1.5$ feeds.

Table 1. Base Case Reactor Operating Conditions

operating conditions	data
reactor diameter	0.026 m
bed height	1.0 m
catalyst density	1982 kg/m^3
voidage of the fixed bed	0.39
catalyst particle diameter	0.002 m
reactor temperature	523 K
reactor pressure	5 MPa
inlet fixed bed superficial gas velocity	0.05 m/s
inlet permeate side superficial velocity	0.1 m/s
membrane area	250 m^2/m$^3_{\text{reactor}}$

Methanol yield was defined as[4]

$$Y_{CH_3OH} = \frac{\dot{F}_{CH_3OH} + 2\dot{F}_{CH_3OCH_3}}{(\dot{F}_{CO} + \dot{F}_{CO_2})_{in}} \quad (42)$$

Over the entire interval of feed compositions, methanol yield increases when CO_2 is gradually replaced with CO. Thus, a negligible synergy effect is observed at high CO_2 content where a relatively large amount of water is produced and the reverse water gas shift reaction is favored. In contrast, a strong synergy is obtained with CO-rich feed due to the effective removal of methanol by dehydration reaction and the product water by WGS. Regardless of CO_2-to-CO proportions, methanol yield as defined by eq 42 is improved through increased H_2/CO_2 ratio.

Figure 2 illustrates the methanol and DME selectivity profiles corresponding to Figure 1 conditions. Methanol and DME selectivities were defined as follows:[9]

$$S_{CH_3OCH_3} = \frac{2\dot{F}_{CH_3OCH_3}}{2\dot{F}_{CH_3OCH_3} + \dot{F}_{CH_3OH}} \quad (43)$$

$$S_{CH_3OH} = \frac{\dot{F}_{CH_3OH}}{2\dot{F}_{CH_3OCH_3} + \dot{F}_{CH_3OH}} \quad (44)$$

DME and methanol selectivity increases/decreases when CO_2 is gradually replaced with CO. The selectivities to methanol or DME are favored at the two opposite extremes of the feed composition range (Figure 2). In a CO-rich environment were dehydration is not affected by water (low water level), DME is the favored product. Conversely, there is a high fraction of unconverted methanol in CO_2-rich feeds where the reverse water

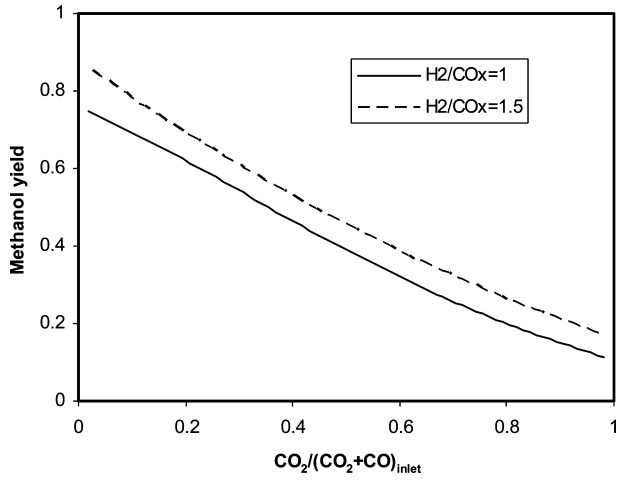

Figure 1. Influence of feed CO_2 fraction on methanol yield (no in situ H_2O removal).

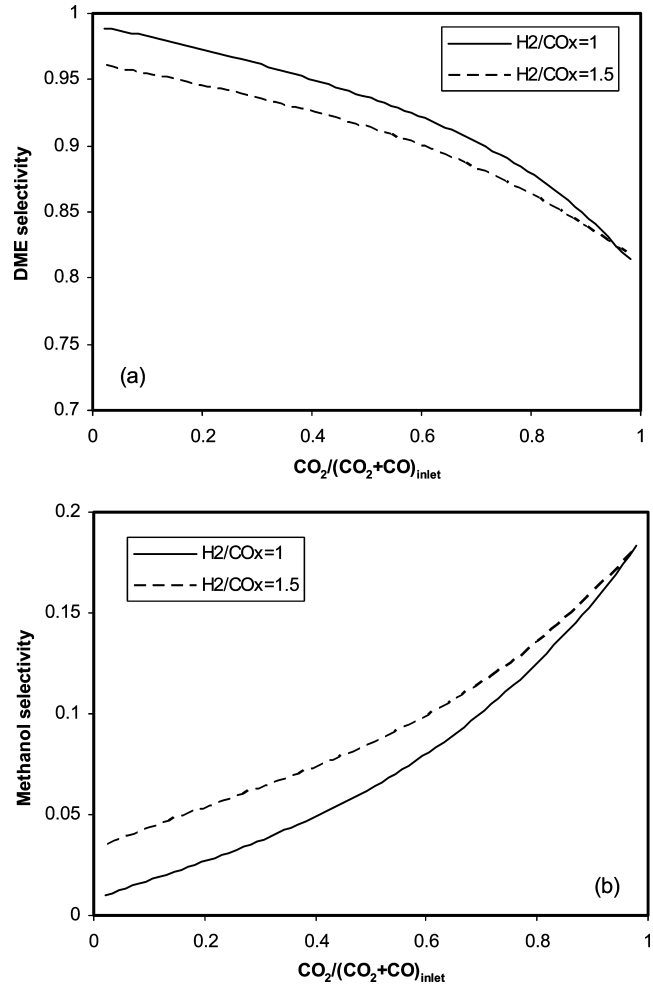

Figure 2. Influence of feed CO_2 fraction on DME (a) and methanol (b) selectivity (no in situ H_2O removal).

gas shift reaction is promoted and dehydration becomes inefficient due to strong water inhibition. The model predicts qualitatively the correct increasing/decreasing trends of DME/methanol selectivity when CO_2 is gradually replaced with CO.[4] In a CO-rich environment, DME selectivity is higher than 95% and is in good agreement with the findings of Lu et al.[9] reported in a fixed-bed reactor.

With the increase of H_2/CO_x ratio, methanol synthesis is promoted leading to higher CO conversion and higher methanol yield and selectivity (Figures 1 and 2). On the contrary, WGS is inhibited by an increasing H_2/CO_x ratio leading thus to less H_2O consumption. Because H_2O is the product of methanol synthesis and dehydration reactions, the increase of H_2/CO_x ratio results in the accumulation of H_2O and a decrease in DME selectivity, Figure 2. The model predicts qualitatively the correct increasing/decreasing trends of methanol/DME selectivity when the H_2/CO_x ratio increases.[4,21]

With in situ H_2O Removal. It appears that without in situ H_2O removal, negligible synergy takes place at high CO_2 content where a relatively large quantity of water is produced and reverse WGS is favored. Therefore, in situ H_2O removal is worth addressing to evaluate its potential and limits in promoting synergistic effects for DME synthesis. The benefit to be expected through H_2O removal is to promote reverse WGS to enhance conversion of CO_2 into methanol (eq 1) and methanol into DME (eq 3).

This section presents simulations under H_2O removal conditions. Figures 3−5 show the influence of in situ H_2O removal

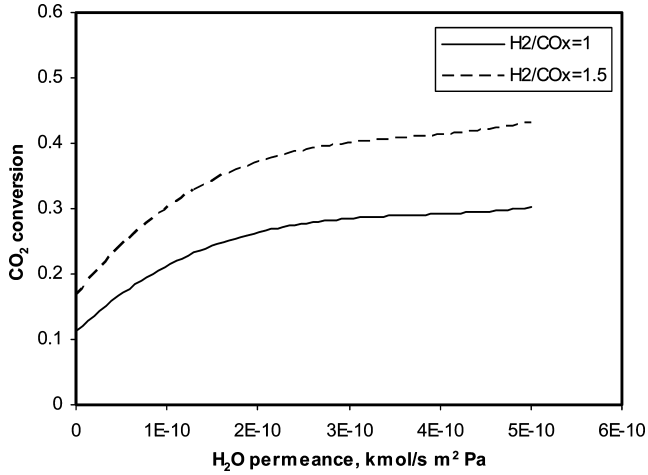

Figure 3. CO_2 conversion as a function of membrane permeance (under in situ H_2O removal). Feed conditions: $H_2/CO_x = 1$; $CO_2 = 49\%$, $CO = 1\%$, $H_2 = 50\%$. $H_2/CO_x = 1.5$; $CO_2 = 39\%$, $CO = 1\%$, $H_2 = 60\%$.

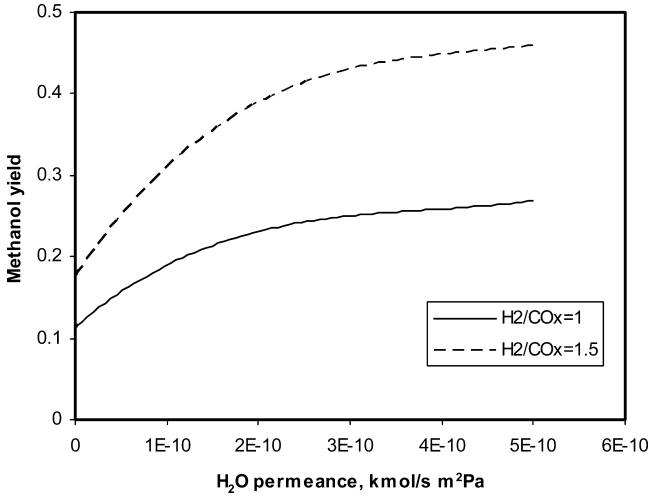

Figure 4. Influence of membrane permeance on methanol yield (under in situ water removal). Feed conditions: $H_2/CO_x = 1$; $CO_2 = 49\%$, $CO = 1\%$, $H_2 = 50\%$. $H_2/CO_x = 1.5$; $CO_2 = 39\%$, $CO = 1\%$, $H_2 = 60\%$.

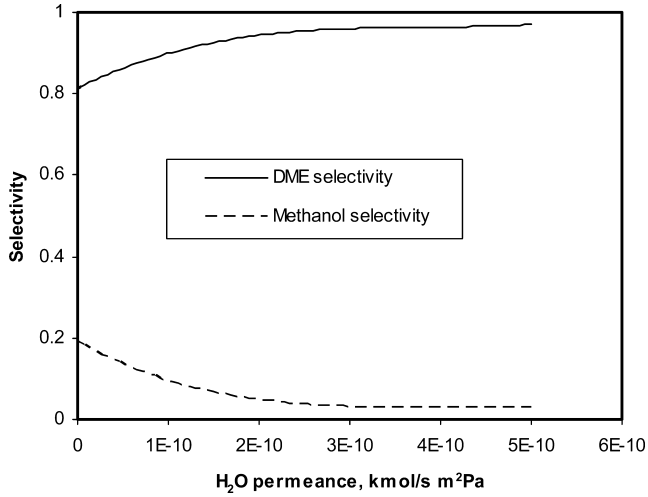

Figure 5. DME and methanol selectivity as a function of membrane permeance (under in situ H_2O removal). Feed conditions: $H_2/CO_x = 1$; $CO_2 = 49\%$, $CO = 1\%$, $H_2 = 50\%$.

at high CO_2 feed concentration on CO_2 conversion, methanol yield, and methanol/DME selectivities. A boost in H_2O membrane permeance favors H_2O-depleted retentate compartment

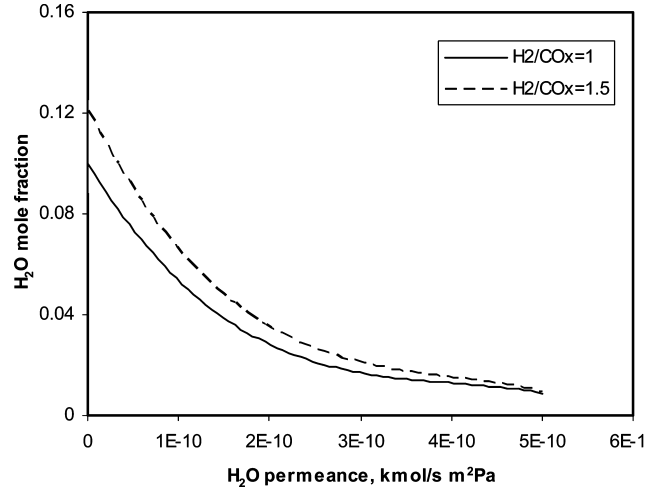

Figure 6. Influence of membrane permeance on exit H_2O fraction (under in situ water removal). Feed conditions: $H_2/CO_x = 1$; $CO_2 = 49\%$, $CO = 1\%$, $H_2 = 50\%$. $H_2/CO_x = 1.5$; $CO_2 = 39\%$, $CO = 1\%$, $H_2 = 60\%$.

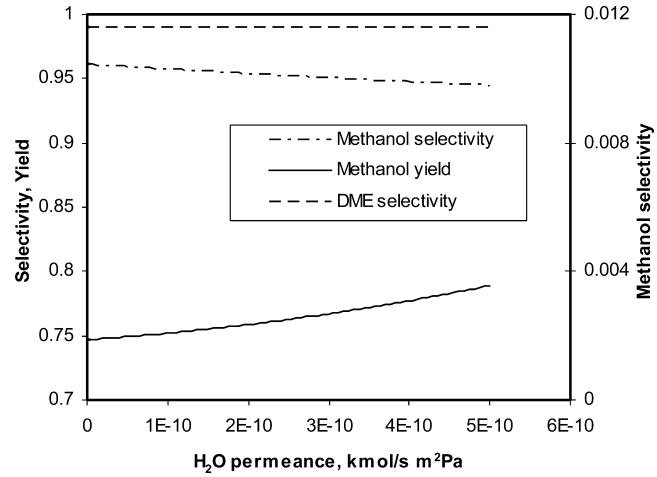

Figure 7. DME and methanol selectivity, methanol yield as a function of membrane permeance (under in situ H_2O removal). Feed conditions: $H_2/CO_x = 1$; $CO = 49\%$, $CO_2 = 1\%$, $H_2 = 50\%$.

due to a high degree of H_2O removal (Figure 6). This translates into a direct positive response in CO_2 conversion (Figure 3) driven by methanol production accelerated by the increased partial pressures of the reactants and by a reduced kinetic inhibition due to H_2O. This is in addition to prompting reverse WGS toward CO formation to result in higher CO partial pressures. Also, with the increase of H_2O membrane permeance and the degree of in situ H_2O removal (Figure 6), the methanol yield is favored (Figure 4), the fraction of unconverted methanol is reduced (Figure 5), and the DME selectivity is favored (Figure 5) as the dehydration reaction is accelerated due to reduced kinetic inhibition by H_2O. By applying this concept, CO_2 can be utilized as a constituent in the synthesis gas as reverse WGS is promoted by in situ H_2O removal.

Figure 7 shows the influence of in situ H_2O removal under high CO feed concentration conditions on the methanol yield and methanol/DME selectivity. Under CO-rich conditions, the methanol yield/ selectivity increases/decreases slowly with increasing H_2O permeance because only a low quantity of water is removable from the reaction system (as opposed to more H_2O resorption by the competing water gas shift reaction itself). The dehydration reaction is not inhibited by water and DME selectivity is not improved significantly with the increase of H_2O permeance.

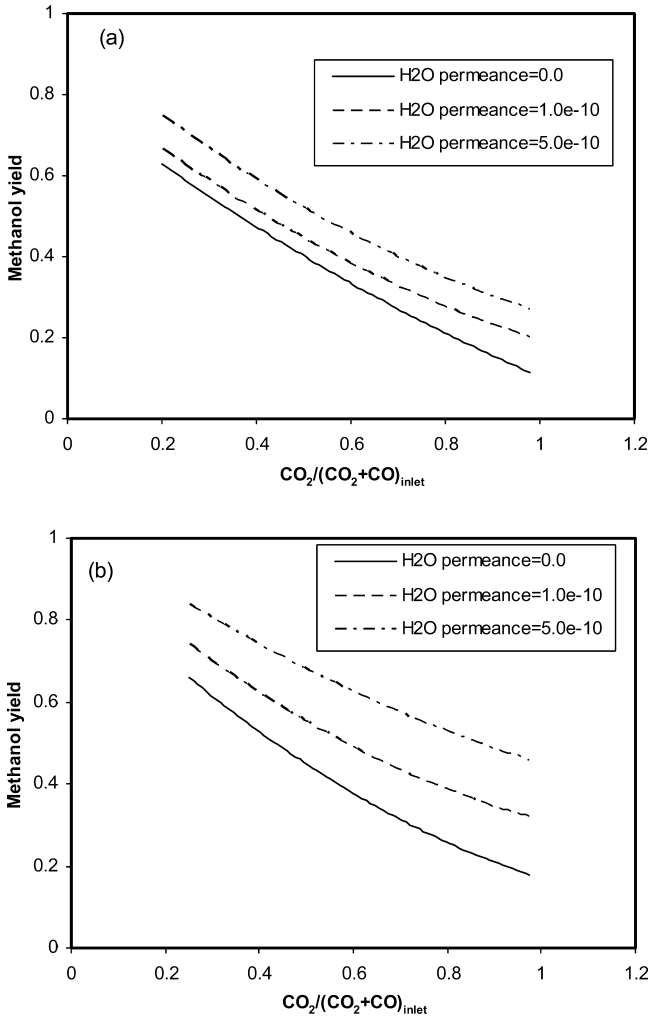

Figure 8. Influence of feed CO_2 fraction and membrane permeance on methanol yield under H_2O removal conditions. Feed conditions: (a) $H_2/CO_x = 1$; $CO_2 + CO = 50\%$, $H_2 = 50\%$. (b) $H_2/CO_x = 1.5$; $CO_2 + CO = 40\%$, $H_2 = 60\%$.

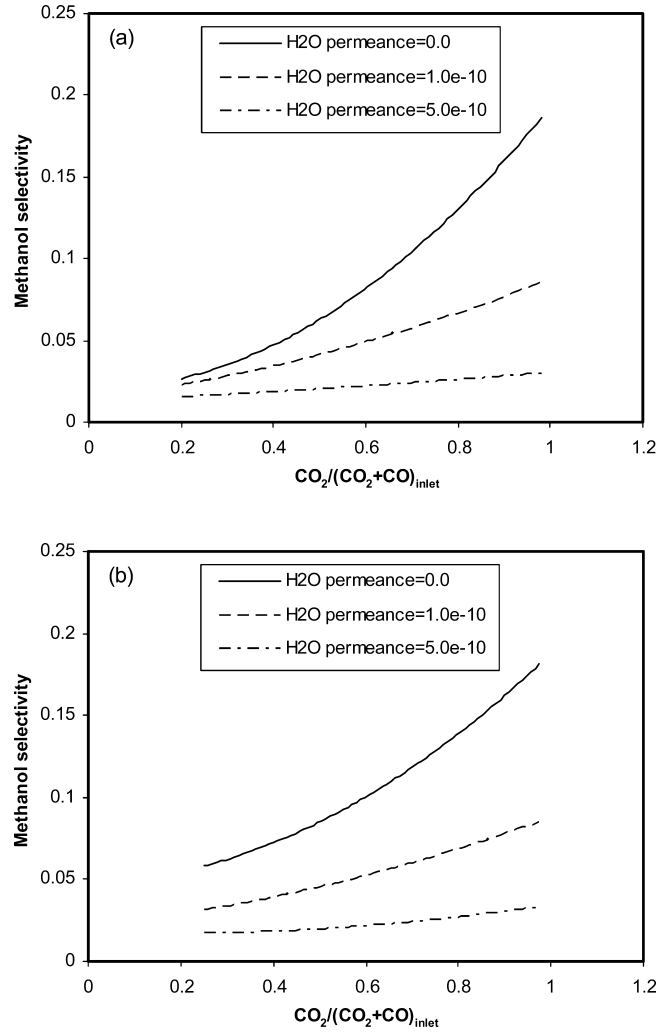

Figure 9. Influence of feed CO_2 fraction and membrane permeance on methanol selectivity under H_2O removal conditions. Feed conditions: (a) $H_2/CO_x = 1$; $CO_2 + CO = 50\%$, $H_2 = 50\%$. (b) $H_2/CO_x = 1.5$; $CO_2 + CO = 40\%$, $H_2 = 60\%$.

It would be also of interest to explore the behavior of DME synthesis under H_2O removal conditions when CO is gradually replaced with CO_2. Figure 8a and b show the influence of H_2O removal on the methanol yield for two different feed compositions: (i) $H_2/CO_x = 1$; $CO_2 + CO = 50\%$, $H_2 = 50\%$. (ii) $H_2/CO_x = 1.5$; $CO_2 + CO = 40\%$, $H_2 = 60\%$. The methanol yield increases with increasing H_2O membrane permeance. This raise becomes more important with the increase of CO_2 feed concentration because a relatively large amount of water is produced followed by a large quantity of water removed from the system (Figure 6). On the other hand, the raise becomes less important when CO feed concentration increases due to the low water level (high amount of H_2O is managed by the water gas shift reaction) and due to the lower quantity of water removed from the reaction system. Under H_2O removal conditions, the increase of methanol yield is higher at higher H_2/CO_x ratios.

Figure 9 shows the influence of H_2O removal on methanol selectivity. With the increase of H_2O membrane permeance and the degree of in situ H_2O removal (Figure 9), the fraction of unconverted methanol is reduced and methanol selectivity decreases. This reduction becomes more important when CO_2 feed concentration increases and the dehydration reaction is favored because a large quantity of water is removed from the reaction system. However, such reduction becomes less important when CO feed concentration increases due to low water level and to lower quantity of water removed from the system. Under H_2O-depleted conditions and CO-rich environment, the decline of methanol selectivity is higher at the higher the H_2/CO_x ratio. On the contrary, under CO_2 rich and H_2O-depleted conditions, methanol selectivity is not influenced by H_2/CO_x ratio.

Figure 10 shows the influence of in situ H_2O removal on the DME yield. DME yield was defined as follows:[4,21]

$$Y_{CH_3OCH_3} = \frac{2\dot{F}_{CH_3OCH_3}}{(\dot{F}_{CO} + \dot{F}_{CO_2})_{in}} \tag{45}$$

As in the case of methanol yield, a boost in H_2O membrane permeance favors in situ H_2O removal and the result is an increase of DME yield. This raise becomes more important with the increase of CO_2 feed concentration because a relatively large amount of water is produced followed by a large quantity of water removed from the system. On the other hand, the raise becomes less important when CO feed concentration increases due to the low water level (the large amount of H_2O is managed by the water−gas shift reaction) and due to the lower quantity of water removed from the reaction system. Under H_2O removal conditions, the increase of DME yield is higher at higher H_2/CO_x ratios.

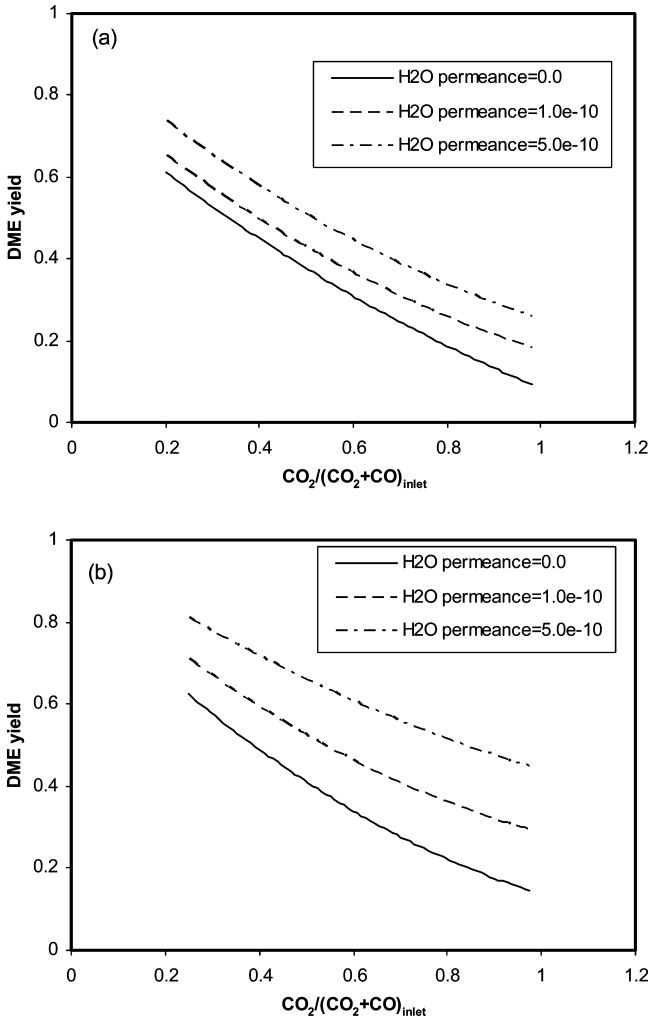

Figure 10. Influence of feed CO_2 fraction and membrane permeance on DME yield under H_2O removal conditions. Feed conditions: (a) $H_2/CO_x = 1$; $CO_2 + CO = 50\%$, $H_2 = 50\%$. (b) $H_2/CO_x = 1.5$; $CO_2 + CO = 40\%$, $H_2 = 60\%$.

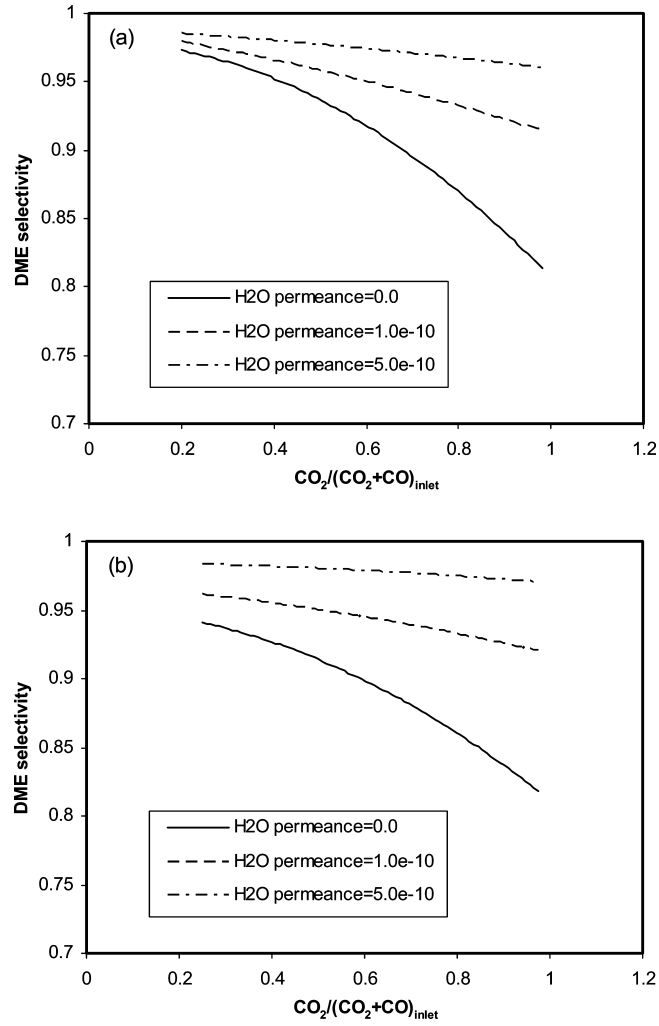

Figure 11. Influence of feed CO_2 fraction and membrane permeance on DME selectivity under H_2O removal conditions. Feed conditions: (a) $H_2/CO_x = 1$; $CO_2 + CO = 50\%$, $H_2 = 50\%$. (b) $H_2/CO_x = 1.5$; $CO_2 + CO = 40\%$, $H_2 = 60\%$.

Figure 11 shows the influence of H_2O removal on DME selectivity. At high H_2O permeance, the dehydration reaction is not inhibited by water and DME selectivity is improved significantly, especially at higher CO_2 feed concentration conditions. Under H_2O removal and higher CO feed content conditions, the improvements in DME selectivity are more important at higher H_2/CO_x ratio.

Conclusion

A chemical reaction engineering model for a fixed-bed membrane reactor was setup to evaluate the potential and limits of the concept of H_2O removal during DME synthesis. The motivation for in situ H_2O removal during DME synthesis by means of hydrophilic membranes is to displace the water−gas shift equilibrium to enhance conversion of CO_2 into methanol and to improve reactor productivity. The following conclusions were drawn from the simulation results:

Under CO rich conditions, only a low quantity of water is removed from the reaction system which results in slow increase/decrease of methanol yield/selectivity with an increase of H_2O permeance. The dehydration reaction is not inhibited by water and DME selectivity is not improved significantly with the increase of H_2O permeance.

When CO is gradually replaced with CO_2, with the increase of H_2O membrane permeance and the extent of in situ H_2O removal, the methanol yield and DME selectivity are favored and the fraction of unconverted methanol is reduced as the dehydration reaction is accelerated due to reduced kinetic inhibition by H_2O. Hence by applying this concept, CO_2 can be utilized as a constituent in the synthesis gas as in situ H_2O removal accelerates the reverse water gas shift reaction.

These preliminary simulation results show that the fixed-bed membrane reactor technology with in situ H_2O removal is more efficient for DME synthesis than a fixed-bed reactor without H_2O removal.

Acknowledgment

Financial support from the Natural Sciences and Engineering Research Council (NSERC) is gratefully acknowledged. F.L. expresses his appreciation to École Centrale de Lille for the visiting professor fellowship.

Nomenclature

a, b = parameters in Peng−Robinson EOS
a_i, b_i = parameters in Peng−Robinson EOS
A = membrane area, m^2
A_i, B_i = parameters in eqs 18−20
C_j = concentration of species j in fixed-bed side, $kmol/m^3$
$\tilde{C}_j$ = concentration of species j in permeate side, $kmol/m^3$

C_g = total concentration of the gas phase in fixed bed side, kmol/m^3
$\tilde{C}_g$ = total concentration of the gas phase in permeate side, kmol/m^3
d_p = particle diameter, m
E_1, E_2 = Ergun constants, −
$\dot{F}$ = mole flux of gas phase in fixed bed side, kmol/(m^2 s)
$\tilde{\dot{F}}$ = mole flux of gas phase in permeate side, kmol/(m^2 s)
$\dot{F}_j$ = mole flux of species j, kmol/(m^2 s)
M_j = molecular mass of species j, kg/kmol
P = reactor pressure in fixed bed side, Pa
$\tilde{P}$ = reactor pressure in fixed bed side, Pa
P_c = critical pressure, Pa
P_j = partial pressure of species j in fixed bed side, Pa
$\tilde{P}_j$ = partial pressure of species j in permeate side, Pa
Q_j = membrane permeance, kmol/(m^2 s Pa)
r_i = reaction rate, kmol/(kg$_{cat}$ s)
R = ideal-gas constant
S_j = selectivity of species j
t = time, s
T = temperature, K
T_c = critical temperature, K
u_g = average interstitial velocity of gas phase in fixed bed side, m/s
$\tilde{u}_g$ = average interstitial velocity of gas phase in permeate side, m/s
v_{sg} = superficial velocity of gas phase in fixed bed side, m/s
V_p = volume of permeate side, m^3
V_r = volume of fixed bed side, m^3
y_j = mole fraction of species j, −
Y_j = yield of species j, −
z = axial coordinate, m
Z_i = compressibility factor, −
Z_p = compressibility factor of the gas in permeate side, −
Z_r = compressibility factor of the gas in fixed-bed side, −

Greek Letters

ε_g = gas holdup in fixed bed side, −
$\tilde{\varepsilon}_g$ = gas holdup in permeate side, −
κ_{ij} = binary interaction parameters
μ_g = gas phase dynamic viscosity in fixed bed side, kg/(m s)
ρ_g = density of gas phase in fixed bed side, kg/m^3
$\tilde{\rho}_g$ = density of gas phase in permeate side, kg/m^3
ρ_{sc} = catalyst bed density, kg/m^3
ω = acentric factor, −

Subscripts

p = permeate
r = retentate

Literature Cited

(1) Toseland, B. A.; Underwood, R. P.; Waller, F. J. Catalyst activity maintenance study for the liquid phase dimethyl ether process. *Proceedings of the DOE Contracts' Review Conference*, Pittsburgh, PA, 1994; pp 307−321.

(2) Bussche, K. M. V.; Froment, G. F. A steady-state kinetic model for methanol synthesis and water gas shift reaction on a commercial Cu/ZnO/Al_2O_3 catalyst. *J. Catal.* **1996**, *161*, 1–10.

(3) Dybkjaer, L.; Hansen, J. B. Large scale production of alternative synthetic fuels from natural gas. In *Natural Gas Conversion IV*; Pontes, M. D. Eds.; Elsevier Science B.V.: Amsterdam, 1997; pp 99−116.

(4) Ng, K. L.; Chadwick, D.; Toseland, B. A. Kinetics and modelling of dimethyl ether synthesis from synthesis gas. *Chem. Eng. Sci.* **1999**, *54*, 3587–3592.

(5) Wang, Z. L.; Wang, J. F.; Diao, J.; Jin, Y. The synergy effect of process coupling dimethyl ether synthesis in slurry reactors. *Chem. Eng. Technol.* **2001**, *24*, 507–515.

(6) Peng, X. D.; Toseland, B. A.; Tijm, P. J. A. Kinetic understanding of the chemical synergy under LPDME conditions-once-through applications. *Chem. Eng. Sci.* **1999**, *54*, 2787–2792.

(7) Peng, X. D.; Wang, A. W.; Toseland, B. A.; Tijm, P. J. A. Single-step syngas-to-dimethyl ether processes for optimal productivity, minimal emissions, and natural gas-derived syngas. *Ind. Eng. Chem. Res.* **1999**, *38*, 4381–4388.

(8) Xiao, W. D.; Lu, W. Z. *A novel technology of DME synthesis from syngas*. Patent no. CN1332141, 2002.

(9) Lu, W.-Z.; Teng, L.-H.; Xiao, W.-D. Simulation and experiment study of dimethyl ether synthesis from syngas in a fluidized bed reactor. *Chem. Eng. Sci.* **2004**, *59*, 5455–5464.

(10) Rohde, M. P.; Schaub, G.; Khajavi, S.; Jansen, J. C.; Kapteijn, F. Fischer−Tropsch synthesis with in situ H_2O removal - Directions of membrane development. *Microporous Mesoporous Mater.* **2008**, *115*, 126–136.

(11) Hu, J.; Wang, Y.; Cao, C.; Elliott, C.; Stevens, D. J.; White, J. F. Conversion of biomass syngas to DME using a microchannel reactor. *Ind. Eng. Chem. Res.* **2005**, *44*, 1722–1727.

(12) Shen, W. J.; Jun, K. W.; Choi, H. S.; Lee, K. W. Thermodynamic investigation of methanol and dimethyl ether synthesis from CO_2 hydrogenation. *Korean J. Chem. Eng* **2000**, *17*, 210–216.

(13) Aguayo, A. T.; Erena, J.; Mier, D.; Arandes, J. M.; Olazar, M.; Bilbao, J. Kinetic modelling of dimethyl ether synthesis in a single step on a CuO-ZnO-Al2O3/gamma-Al_2O_3 catalyst. *Ind. Eng. Chem. Res.* **2007**, *46*, 5522–5530.

(14) Erena, J.; Sierra, I.; Olazar, M.; Gayubo, A. G.; Aguayo, A. T. Deactivation of a CuO-ZnO-Al_2O_3/gamma-Al_2O_3 catalyst in the synthesis of dimethyl ether. *Ind. Eng. Chem. Res.* **2008**, *47*, 2238–2247.

(15) Espinoza, R.; du Toit, E.; Santamaria, J.; Menendez, M.; Coronas, J.; Irusta, S. Use of membranes in Fischer−Tropsch reactors. *Stud. Surf. Sci. Catal.* **2000**, *130*, 389–395, Part 1.

(16) Rohde, M. P.; Unruh, D.; Schaub, G. Membrane application in Fischer−Tropsch synthesis to enhance CO_2 hydrogenation. *Ind. Eng. Chem. Res.* **2005**, *44*, 9653–9661.

(17) Unruh, D. *Fischer−Tropsch Synthese mit Synthesegasen aus Biomasse - Verbesserung der Kohlenstoffnutzung durch Anwendung eines Membranreaktors*; Shaker: Aachen, 2006.

(18) Reid, R. C.; Prausnitz, J. M.; Poling, B. E. *The properties of gases and liquids*, 4th ed.; McGraw Hill: New York, 1987.

(19) Herman, R. G.; Klier, K. J. Catalytic synthesis of methanol from carbon monoxide/hydrogen. *J. Catal.* **1979**, *56*, 407–429.

(20) Zhang, H. T.; Cao, F. H.; Liu, D. H.; Fang, D. Y. Thermodynamic analysis for synthesis of dimethyl ether and methanol from synthesis gas. *J. ECUST.* **2001**, *27*, 198–201.

(21) Erena, J.; Garona, R.; Arandes, J. M.; Aguayo, A.; Bilbao, J. Direct synthesis of dimethyl ether from (H_2+CO) and (H_2+CO_2) feeds. Effect of feed composition. *Int. J. Chem. React. Eng.* **2005**, *3*, 44.

Received for review November 1, 2009
Revised manuscript received January 20, 2010
Accepted January 25, 2010

IE901726U